Journal of Sound and Vibration (1997) **199**(1), 33–50

DYNAMIC BEHAVIOUR OF MULTI-SPAN BEAMS UNDER MOVING LOADS

K. Henchi, M. Fafard

GIREF, Department of Civil Engineering, Laval University, Quebec G1K 7P4, Canada

G. Dhatt

GIREF, Department of Mechanical Engineering, INSA de Rouen, 76130 Mont-Saint-Aignan, France

AND

M. Talbot

Ministry of Transportation, Bridge Division, Quebec G1S 4X9, Canada

(*Received* 26 *February* 1996, *and in final form* 10 *May* 1996)

In this paper, an exact dynamic stiffness element under the frame work of finite element approximation is presented to study the dynamic response of multi-span structures under a convoy of moving loads. A dynamic model coupled with a FFT algorithm is developed. The model is highly efficient for calculating the response of bridges under multiaxle moving forces. All the vibration frequencies and mode shapes of the beam-structure may be calculated exactly using the Wittrick and Williams algorithm. Examples show that with only one element per span, exact frequencies and modes could be obtained. Some results on the dynamic amplification factor are presented also as a function of the speed of the moving loads.

1. INTRODUCTION

The investigation of dynamic behaviour of beam-structures under moving loads has been a topic of interest for well over a century. A few studies were made on the problem of the vibration of simple and continuous beams under moving loads and are available in the textbook of Fryba [1]. Hayashikawa and Watanabe [2] apply the continuum method of dynamic analysis to multi-span continuous beam under a concentrated moving load. Due to new developments in rapid transport systems (fast trains, trucks with multiple containers, etc.), it has become essential to study the behaviour of bridges under moving loads at various speeds. Moreover, due to high strength materials, bridge structures have become lighter with longer spans, therefore requiring detailed consideration of high frequency models.

Before undertaking dynamic analysis, it is desirable to obtain an estimate of natural modes and frequencies of the bridge. One can employ traditional finite element models to obtain these [3, 4]. However for beam structures, finite element models based on exact dynamic expressions lead to higher precision with only one element per span [2, 5, 6]. The dynamic response under multiple moving loads may be obtained by a direct integration technique coupled with finite element discretization. However, such an approach may become very cumbersome and imprecise for moving loads at speeds near the resonance frequencies of the bridge structure. It is thus common to use the modal technique to obtain

0022–460X/97/010033 + 18 $25.00/0/sv960628

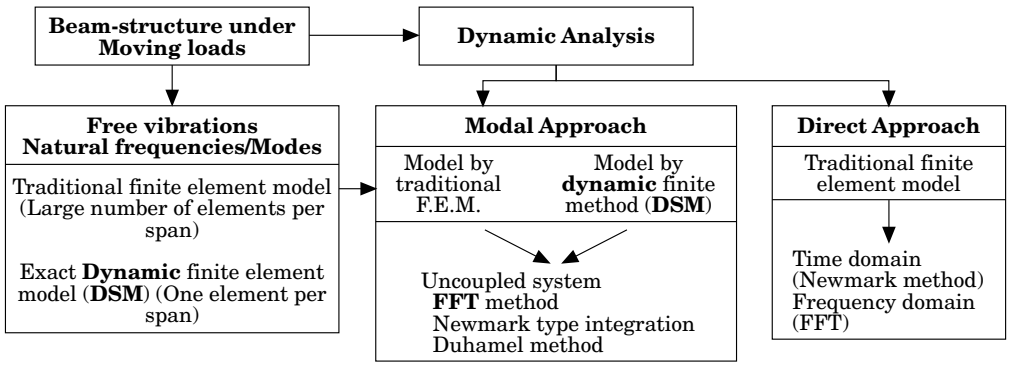

Figure 1. Dynamic analysis procedure of beam-structure systems under moving loads.

the uncoupled system of equations which are solved by direct integration [3]. One may also employ the FFT technique [3, 7] to obtain the solution of uncoupled system with multiple moving loads [8, 9].

In this study, the modal technique is used coupled with an FFT algorithm to obtain the dynamic response of continuous bridges. The contribution of the present study relates to the utilisation of an exact dynamic approach coupled with the FFT technique for studying the dynamic response of beam structures under multiple moving loads. A summary of different solution techniques is presented in Figure 1.

In section 2, a dynamic finite element formulation is presented, followed by the modal FFT approach. Three examples will be presented to demonstrate the efficiency of the new model developed in this paper.

2. DYNAMIC FINITE ELEMENT MODEL

2.1. VARIATIONAL FORMULATION

A beam-type structure is composed of beam elements interconnected at their end points (Figure 2). The interest of this study is the development of a model of multi-span beam structures. The weak formulation of virtual work expression of transverse vibration of Bernoulli-Euler beams under moving loads is [10, 11, 12]

$$W = \int_0^L (\delta w m_l w_{,tt} + \delta w c w_{,t} + \delta w_{,xx} EI w_{,xx})\,\mathrm{d}x - \int_0^L \delta w P(x, t)\,\mathrm{d}x = 0, \qquad \forall \delta w, \qquad (1)$$

where w is the transverse displacement, $w_{,xx}$, $w_{,t}$ are the spatial and temporal derivations of w, $\delta w(x)$ is the virtual displacement or test function, m_l is the mass per unit of length of the beam, c is the damping coefficient, E is the modulus of elasticity, I is the second moment of area for the beam's cross-section and $P(x, t)$ is the moving load distribution

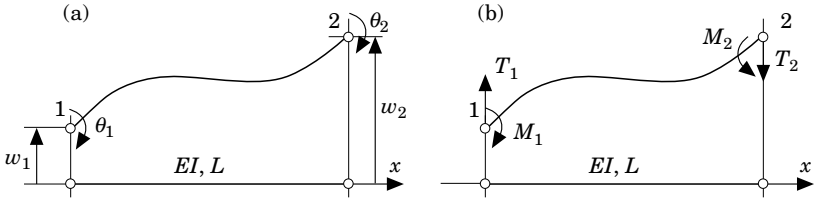

Figure 2. A bending beam element: (a) end displacement, (b) end forces.

equal to $\delta(x - x_i)F_i$ where x_i is the position of the moving concentrated moving load i and $\delta(x - x_i)$ is the Dirac delta function. It is assumed here that applied moments at both ends of beam are zero.

The weak formulation for free vibration is obtained by considering $c = 0$ and $P(x, t) = 0$ and

$$w(x, t) = w(x)\,\mathrm{e}^{\mathrm{i}\omega t}; \qquad \delta w = \delta w(x), \tag{2}$$

$$W = \int_0^L (-\delta w m_l \omega^2 w + \delta w_{,xx} EI w_{,xx})\,\mathrm{d}x = 0, \qquad W = EI \int_0^L (\delta w_{,xx} w_{,xx} - \delta w \alpha^4 w)\,\mathrm{d}x = 0 \tag{3}$$

with $\alpha^4 = m_l\omega^2/EI$. For a structure discretized by finite elements, equation (3) is written as

$$W = \sum W^e = 0. \tag{4}$$

The finite element discretization is obtained by choosing a C^1 approximation for w and δw:

$$w(x) = \sum_{i=1,4} N_i(x, \alpha) w_i, \qquad \delta w(x) = \sum_{i=1,4} N_i(x, \alpha)\delta w_i, \tag{5}$$

where EI, m_l are constant per element and $w_1 = w(x = 0)$, $w_2 = \theta(x = 0) = -w_{,x}(x = 0)$, $w_3 = w(x = L)$, $w_4 = \theta(x = L) = -w_{,x}(x = L)$. The traditional finite element model is obtained by choosing a Hermite type polynomial approximation (Dhatt and Touzot [13], Bathe [14]).

2.2. DYNAMIC STIFFNESS MATRIX (DSM)

For the dynamic finite element model, the nodal approximation N_i is chosen such that

$$\delta w_{,xxxx} - \alpha^4 \delta w = 0, \qquad \langle N_{i,xxxx} - \alpha^4 N_i \rangle \{\delta w_i\} = 0, \tag{6}$$

where N_i satisfy the following conditions at each node:

$$\begin{aligned}
&N_1(x = 0) = 1, \quad N_1(x = L) = 0, \quad N_{1,x} = 0 \quad \text{at} \quad x = 0, L;\\
&N_3(x = 0) = 0, \quad N_3(x = L) = 1, \quad N_{3,x} = 0 \quad \text{at} \quad x = 0, L;\\
&N_{2,x}(x = 0) = 1, \quad N_{2,x}(x = L) = 0, \quad N_2 = 0 \quad \text{at} \quad x = 0, L;\\
&N_{4,x}(x = 0) = 0, \quad N_{4,x}(x = L) = 1, \quad N_4 = 0 \quad \text{at} \quad x = 0, L.
\end{aligned}$$

The expression W^e may be written in the following equivalent form after two integrations by parts of equation (3):

$$W^e = EI \int_0^L (\delta w_{,xxxx} - \alpha^4 \delta w) w\,\mathrm{d}x - EI[\delta w_{,xx} w_{,x}]_0^L + EI[\delta w_{,xxx} w]_0^L$$

or

$$W^e = EI \int_0^L (w_{,xxxx} - \alpha^4 w)\delta w\,\mathrm{d}x - EI[w_{,xx}\delta w_{,x}]_0^L + EI[w_{,xxx}\delta w]_0^L. \tag{7}$$

The approximation satisfying equation (6) leads to a finite element model which gives exact results as it may be deduced from equation (7) since the integral term becomes zero. The approximation of N_i functions is obtained as follows:

$$w(x) = \langle P(\alpha, x)\rangle\{c\} \tag{8}$$

with $\langle P(\alpha, x)\rangle = \langle \cos \alpha x \sin \alpha x \cosh \alpha x \sinh \alpha x\rangle$ where each term satisfies equation (6). The coefficients c_i are transformed by w_i by using relations defined after equation (5):

$$\begin{Bmatrix} c_1 \\ c_2 \\ c_3 \\ c_4 \end{Bmatrix} = \begin{bmatrix} 1 & 0 & 1 & 0 \\ 0 & -\alpha & 0 & -\alpha \\ \cos \alpha L & \sin \alpha L & \cosh \alpha L & \sinh \alpha L \\ \alpha \sin \alpha L & -\alpha \cos \alpha L & -\alpha \sinh \alpha L & -\alpha \cosh \alpha L \end{bmatrix}^{-1} \begin{Bmatrix} w(0) \\ \theta(0) \\ w(L) \\ \theta(L) \end{Bmatrix}. \tag{9}$$

The N_i functions defined in equation (5) are finally obtained from equations (8) and (9) and they satisfy equation (6):

$$\langle N(\alpha, x)\rangle = \langle P(\alpha, x)\rangle[P_n]^{-1}. \tag{10}$$

The expression W^e of equation (7) and the corresponding discretized form can be written as

$$W^e = EI\langle \delta w(x=0) \quad -\delta w_{,x}(x=0) \quad \delta w(x=L) \quad -\delta w_{,x}(x=L)\rangle \begin{Bmatrix} -w_{,xxx}(x=0) \\ -w_{,xx}(x=0) \\ w_{,xxx}(x=L) \\ w_{,xx}(x=L) \end{Bmatrix},$$

$$W^e = \langle \delta w_n\rangle[\mathrm{k}_d(\omega^2)]\{w_n\} = \langle \delta w_n\rangle \begin{Bmatrix} T_1 \\ M_1 \\ T_2 \\ M_1 \end{Bmatrix}, \tag{11}$$

where

$$T(x) = -EIw_{,xxx}, \qquad M(x) = -EIw_{,xx}, \qquad T_1 = T(x=0), \qquad T_2 = -T(x=L),$$
$$M_1 = M(x=0), \qquad M_2 = -M(x=L). \tag{12}$$

The matrix $[\mathrm{k}_d(\omega^2)]$ is defined by

$$\begin{Bmatrix} T_1 \\ M_1 \\ T_2 \\ M_2 \end{Bmatrix} = EI \begin{bmatrix} -N_{1,xxx}(0) & -N_{2,xxx}(0) & -N_{3,xxx}(0) & -N_{4,xxx}(0) \\ -N_{1,xx}(0) & -N_{2,xx}(0) & N_{3,xx}(0) & -N_{4,xx}(0) \\ N_{1,xxx}(L) & N_{2,xxx}(L) & N_{3,xxx}(L) & N_{4,xxx}(L) \\ N_{1,xx}(L) & N_{2,xx}(L) & N_{3,xx}(L) & N_{4,xx}(L) \end{bmatrix} \begin{Bmatrix} w_1 \\ \theta_1 \\ w_2 \\ \theta_2 \end{Bmatrix}$$

$$= [\mathrm{k}_d(\omega^2)]\{w_n\} \tag{13}$$

with $\langle N_{,xxx}\rangle = \langle P_{,xxx}\rangle[P_n]^{-1}$ and $\langle N_{,xx}\rangle = \langle P_{,xx}\rangle[P_n]^{-1}$. The dynamic stiffness matrix of each element is given by equation (13) and in appendix A.

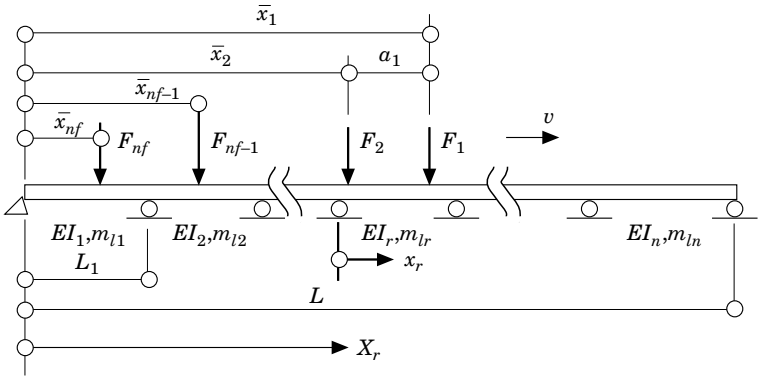

Figure 3. Multi-span bridge—N span continuous beam.

2.3. FREE VIBRATION

After assembling and elimination of rows and columns corresponding to the boundary conditions, the free vibration problem becomes

$$[\mathrm{K}_d(\omega^2)]\{\mathrm{U}_n\} = \{0\}, \qquad [\mathrm{K}(\omega^2) - \omega^2 M(\omega^2)] \,.\, \{\mathrm{U}_n\} = \{0\}, \tag{14}$$

where $[M(\omega^2)]$ is approximated by a first order linearization [15] of $[\mathrm{K}_d(\omega^2)]$:

$$[M(\omega^2)] = -\partial[\mathrm{K}_d(\omega^2)]/\partial\omega^2.$$

The solution of this non-linear eigenvalue problem (equation (14)) is performed using the Wittrick and Williams algorithm [16]. To determine the undamped frequency ω_n for the continuous beam-structure, the number $n(\omega^*)$ of frequencies of this structure exceeded by a fixed trial frequency ω^*, is given by

$$n(\omega^*) = n_0(\omega^*) + s\{\mathrm{K}_d(\omega^*)\}, \tag{15}$$

where $n_0(\omega^*)$ is the number of frequencies exceeded by ω^* if all degrees of freedom of the structure are clamped (displacements being constrained to zero) [12, 16, 17] and $s\{\mathrm{K}_d(\omega^*)\}$ is the number of negative diagonal elements in the triangulated dynamic stiffness $[\mathrm{K}_d(\omega^*)]$ evaluated at $\omega = \omega^*$. An iterative method such as the bisection method is used in order to converge to the true frequency [17].

One may remark that the discretized model contains one element per span and it leads to an exact evaluation of the complete frequency spectrum and the mode shapes of the bridge structure. Corresponding to each frequency ω, mode shapes of the rth span are defined by

$$\phi_{jr}(x_r) = A_{jr}\cos(\alpha_{jr}x_r) + B_{jr}\sin(\alpha_{jr}x_r) + C_{jr}\cosh(\alpha_{jr}x_r) + D_{jr}\sinh(\alpha_{jr}x_r) \tag{16}$$

or

$$\phi_{jr}(x_r) = \sum_{i=1,4} N_i(\alpha_j, x_r)\phi_{jr}^i,$$

where ϕ_{jr} is the jth mode shape of the rth span (see Figure 3) and x_r is the local co-ordinate of the span r. The jth mode shape of the total structure is defined by $\Phi_j(X_r) = \phi_{jr}(x_r)$ where

$$X_r = x_r + \sum_{i=1,r-1} l_i.$$

When an element is clamped, $\{w_n\} = \{0\}$, the vibration mode is defined by

$$w(x_r) = \phi_{jr}(x_r) = \sum P_i(x_r, \alpha_j)c_i, \qquad i = 1, 4 \text{ for span } r.$$

2.4. MODAL REPRESENTATION

The representation of equation (1) in modal space leads to a set of uncoupled relations. Let the nodal vector $\{w\}$ be expressed in modal space by

$$\{w\} = \sum_{j=1,n} \{\Phi_j(X_r)\}y_j(t); \qquad \{\delta w\} = \sum_{j=1,n} \{\Phi_j(X_r)\}\delta y_j(t), \tag{17}$$

where $\{\Phi_j\}$ is the eigenvector satisfying $[\mathrm{K}_d(\omega_j)]\{\Phi_j\} = \{0\}$. For each element, the modal representation of transverse deflection is

$$w(x_r, t) = \sum_{j=1,n} \Phi_j(X_r)y_j(t) = \sum_{j=1,n} \left(\sum_{i=1,4} N_i(\alpha_j, x_r)\phi_{jr}^i \right) y_j(t), \tag{18}$$

where ϕ_{jr}^i are the nodal displacements for the element (span) r, relative to the mode j. The orthogonal properties of modes are verified by writing equation (7) for modes (m, p) with test functions relative to (p, m):

$$W^{m-p} = \sum_{r=l,nspan} \left(\int_0^{l_r} (\Phi_{p,xx}EI\Phi_{m,xx} - \omega_m^2\Phi_p m_l \Phi_m)\, \mathrm{d}x \right) = 0,$$

$$W^{p-m} = \sum_{r=l,nspan} \left(\int_0^{l_r} (\Phi_{m,xx}EI\Phi_{p,xx} - \omega_p^2\Phi_m m_l \Phi_p)\, \mathrm{d}x \right) = 0, \tag{19}$$

or

$$\int_0^{L_T} (\Phi_{m,xx}EI\Phi_{p,xx})\, \mathrm{d}x = 0; \qquad \int_0^{L_T} (\Phi_m m_l \Phi_p)\, \mathrm{d}x = 0 \qquad \text{for } p \neq m, \tag{20}$$

where l_r is the length of the span r and $L_T = \Sigma\, l_r$ is the total length of the beam structure. One may remark that modes $\{\Phi_j\}$ are not orthogonal with respect to $[\mathrm{K}(\omega^2)]$ and $[\mathrm{M}(\omega^2)]$ as in the case of a classical finite element model. The modal representation of equation (1) becomes for each mode j and $\forall \delta y_j$

$$W^{(j)} = \delta y_j \int_0^{L_T} ((\Phi_j m_l \Phi_j)y_{j,tt} + (\Phi_j c \Phi_j)y_{j,t} + (\Phi_{j,xx}EI\,\Phi_{j,xx})y_j)\, \mathrm{d}x$$

$$- \delta y_j \int_0^{L_T} \Phi_j P(x, t)\, \mathrm{d}x = 0. \tag{21}$$

By considering that (reference [2]),

$$\int_0^{L_T} (\Phi_j^2)\, \mathrm{d}x = M_j^2 = \sum_{r=1,nspan} \frac{l_r}{2} (A_{jr}^2 + B_{jr}^2 + C_{jr}^2 - D_{jr}^2) \tag{22}$$

and using equations (22) in (21), one obtains

$$\ddot{y}_j(t) + 2\xi_j\omega_j\dot{y}_j + \omega_j^2 y_j = \Delta_{jr}\int_0^{L_T} \Phi_j \sum_{i=1}^{nl} \delta(x - \bar{x}_i)F_i \, \mathrm{d}x, \tag{23}$$

where

$$\Delta_{jr} = 1/(m_{l_r}M_j^2),\ c/m_{l_r} = 2\xi_j\omega_j \text{ and } \sum_{i=1}^{nl} \delta(x - \bar{x}_i)F_i$$

is the Dirac representation of the moving loads along the bridge, where F_i could be given in the general form as

$$F_i(t) = F_{0i} + F_{1i}\sin(\omega_i t + \phi_i).$$

The transverse deflection of the rth span at x_r (local position in the rth span) is given by

$$w(x_r, t) = \sum_{j=1}^{nmode} \phi_{jr}(x_r)y_j(t). \tag{24}$$

The development of the second term of equation (23) gives the generalized load $p_j(t)$ of mode j,

$$\Delta_{jr}\int_0^{L_T} \Phi_j \sum_{i=1}^{nl} \delta(x - \bar{x}_i)F_i \, \mathrm{d}x = \Delta_{jr}\sum_{p=1}^{nspan}\left(\int_0^{l_p} \phi_{jp} \sum_{i=1}^{nl} \delta(x - \bar{x}_i)F_i \, \mathrm{d}x\right)$$

$$= \Delta_{jr}\sum_{i=1}^{nl} \Phi_j(\bar{x}_i)F_i = p_j(t). \tag{25}$$

If the load F_i is on the span m (Figure 4), one has

$$\Phi_j(\bar{x}_i)F_i = \phi_{jm}(x_m)F_i, \tag{26}$$

where

$$x_m = \bar{x}_i - \sum_{r=1}^{m-1} l_r$$

and $\bar{x}_i$ is given in function of the position of the first load by

$$\bar{x}_i = \bar{x}_1 - \sum_{j=1}^{i-1} a_j,$$

with a_j defined as the relative position between the loads F_j and F_{j-1} (Figure 3).

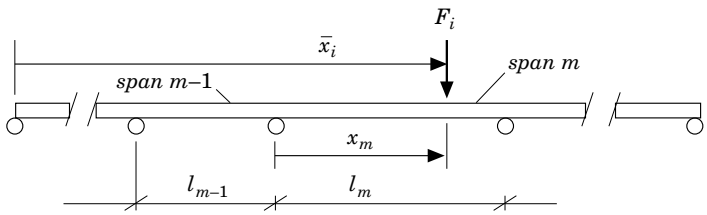

Figure 4. Identification of the local position x_m of the load F_i in the span m.

The solution of linear equation (23) could be obtained using the Duhamel integral

$$y_j(t) = \int_0^t p_j(\tau) h(t-\tau)\,\mathrm{d}\tau + \Theta_0(t), \tag{27}$$

where $h(t-\tau)$ is the response of the structure to an impulse of unit magnitude applied at time $t = \tau$:

$$h(t-\tau) = (e^{-\xi_j\omega_j(t-\tau)}/\omega_d)\sin(\omega_d(t-\tau)), \tag{28}$$

where $\omega_d = \omega_j\sqrt{1-\xi_j^2}$. The solution due to the initial conditions is given by

$$\Theta_0(t) = e^{-\xi_j\omega_j}(y_j(0)\cos(\omega_d) + ((\dot{y}_j(0) + \xi_j\omega_j y_j(0))/\omega_d)\sin(\omega_d t)). \tag{29}$$

2.5. FREQUENCY DOMAIN RESPONSE

The solution can be more easily obtained by transforming equation (23) into the frequency domain using the Fourier transform technique [8, 4]:

$$P_f(\Omega) = \int_{-\infty}^{+\infty} p(t)\,\mathrm{e}^{-\mathrm{i}\Omega t}\,\mathrm{d}t, \qquad Y_f(\Omega) = \int_{-\infty}^{+\infty} y(t)\,\mathrm{e}^{-\mathrm{i}\Omega t}\,\mathrm{d}t,$$

$$\mathrm{i}\Omega Y_f(\Omega) = \int_{-\infty}^{+\infty} \dot{y}(t)\,\mathrm{e}^{-\mathrm{i}\Omega t}\,\mathrm{d}t, \qquad -\Omega^2 Y_f(\Omega) = \int_{-\infty}^{+\infty} \ddot{y}(t)\,\mathrm{e}^{-\mathrm{i}\Omega t}\,\mathrm{d}t. \tag{30}$$

Using equations (30), equation (23) becomes

$$(-\Omega^2 + \mathrm{i}\Omega 2\xi_j\omega_j + \omega_j^2)Y_f(\Omega) = P_f(\Omega)$$

and thus the solution in the frequency domain is

$$Y_f(\Omega) = H_f(\Omega)\cdot P_f(\Omega), \tag{31}$$

where the transfer function is given by

$$H_f(\Omega) = 1/(-\Omega^2 + 2\mathrm{i}\Omega\xi_j\omega_j + \omega_j^2).$$

The solution in the time domain is obtained by the inverse transform as follows:

$$y_j(t) = \frac{1}{2\pi}\int_{-\infty}^{+\infty} Y_f(\Omega)\,\mathrm{e}^{\mathrm{i}\Omega t}\,\mathrm{d}\Omega, \qquad \dot{y}_j(t) = \frac{1}{2\pi}\int_{-\infty}^{+\infty} \mathrm{i}\Omega Y_f(\Omega)\,\mathrm{e}^{\mathrm{i}\Omega t}\,\mathrm{d}\Omega,$$

$$\ddot{y}_j(t) = \frac{1}{2\pi}\int_{-\infty}^{+\infty} -\Omega^2 Y_f(\Omega)\,\mathrm{e}^{-\mathrm{i}\Omega t}\,\mathrm{d}\Omega. \tag{32}$$

Considerations of initial conditions are presented in section 3.

3. DISCRETE FOURIER TRANSFORM

The dynamic finite element model leads to an exact evaluation of frequencies and modes (ω_j, Φ_j). The dynamic response of multi-span beam-structure can be reduced to a numerical solution of equations (31) and (32) for each mode j using the discrete Fourier transform.

The discrete evaluation of $P_f(\Omega)$ is

$$P_f(n\Delta\Omega) = \Delta t \sum_{k=0}^{N-1} p(k\Delta t)\, e^{-2\pi i k n/N}. \tag{33}$$

One should choose the time period T_2 large enough to cover the response characteristics of the system:

$$\Delta t = T_2/N, \qquad T_2 = T_1 + T, \qquad T_1 \geqslant 2\pi/\omega_1, \tag{34}$$

where T_1 is the fundamental period of the structure and T is the period of the exciting load. In order to discretize the pulsation interval Ω, one uses $\Delta\Omega = 2\pi/T_2$ with $0 \leqslant \Omega \leqslant \Omega_{max} = 2\pi/\Delta t$, where Ω_{max} is the Nyquist pulsation. The choice of Δt is such that $f_s \leqslant 1/2\Delta t$, where f_s is the highest frequency present in the signal and participating in the response of the structure. One should verify that

$$\Delta t \leqslant 1/2f_{max}. \tag{35}$$

The discrete representation requires a judicious choice of T_2 and N which defines Δt, $\Delta\Omega$. One may remark that the time and pulsation are divided into N steps. The response of the structure for each mode is obtained in four steps as explained hereafter.

Step 1: Discrete representation of $P_f(n\Delta\Omega)$.

$$p(k\Delta t) \rightarrow P_f(n\Delta\Omega) = \Delta t \sum_{k=0}^{N-1} p(k\Delta t)\, e^{-2\pi i k n/N}, \qquad n = 0, \ldots, N-1. \tag{36}$$

Evaluate $P_f(0)$, $P_f(1)$, $P_f(n\Delta\Omega)$, ..., $P_f((N-1)\Delta\Omega)$.

Step 2: Discrete evaluation of $H_f(n\Delta\Omega)$.

$$h(k\Delta t) \rightarrow H_f(n\Delta\Omega) = 1/(-(n\Delta\Omega)^2 + i(n\Delta\Omega)2\omega\xi + \omega^2). \tag{37}$$

Step 3: Solution by inverse transform of $Y_f(n\Delta\Omega)$, $n = 0, \ldots, N-1$.

$$Y_f(n\Delta\Omega) = H_f(n\Delta\Omega)P_f(n\Delta\Omega) \rightarrow y(k\Delta t) = \frac{\Delta\Omega}{2\pi} \sum_{k=0}^{N-1} Y_f(n\Delta\Omega)\, e^{ikn\Delta t\Delta\Omega}. \tag{38}$$

Compute the velocity and the acceleration (optional).

$$\dot{y}(k\Delta t) = \frac{\Delta\Omega}{2\pi} \sum_{k=0}^{N-1} in\Delta\Omega\, Y_f(n\Delta\Omega)\, e^{ikn\Delta t\Delta\Omega}, \qquad \ddot{y}(k\Delta t) = \frac{\Delta\Omega}{2\pi} \sum_{k=0}^{N-1} -(n\Delta\Omega)^2 Y_f(n\Delta\Omega)\, e^{ikn\Delta t\Delta\Omega}. \tag{39, 40}$$

The numerical implementation of these three steps is done by using the FFT algorithm [7–9]. The responses $y(k\Delta t)$ and $\dot{y}(k\Delta t)$ obtained in step 3 do not satisfy the initial conditions. In order to obtain the response with correct initial conditions, one simply superimposes the influence of initial conditions using the same technique as presented in equation (29).

Step 4: Corrective transient response based on initial conditions.

By applying the initial conditions to the solution obtained by the FFT algorithm $y(k\Delta t)$ [8, 9], the exact solution is noted by $y^*(k\Delta t)$ and the value $y(0)$ is known, with the initial

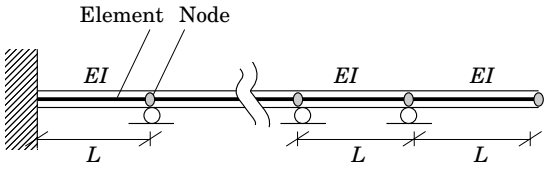

Figure 5. Multi-span beam with one element per span with: $L = 1{\cdot}0$ m, $m_l = 1{\cdot}0$ kg/m, $A = 0{\cdot}01$ m^2, $I = 8{\cdot}33 \times 10^{-6}$ m^4 and $E = 12{\cdot}0 \times 10^4$ N/m^2.

velocity given by

$$\dot{y}(0) = -\frac{\Delta\Omega^2}{\pi} \sum_{k=0}^{N-1} n \, \mathrm{Im}\, \{Y_f(n\Delta\Omega)\}. \tag{41}$$

The difference between the initial conditions in the transient and periodic responses can be evaluated by

$$\Delta y(0) = y^*(0) - y(0), \qquad \Delta\dot{y}(0) = \dot{y}^*(0) - \dot{y}(0), \tag{42}$$

where $r(t)$ is the transient response due to a unit displacement at $t = 0$:

$$r(t) = \mathrm{e}^{-\xi\omega t} (\cos(\omega_d t) + \xi\omega \sin(\omega_d t)/\omega_d), \tag{43}$$

and $s(t)$ is the transient response due to a unit velocity at $t = 0$:

$$s(t) = \mathrm{e}^{-\xi\omega t} \sin(\omega_d t)/\omega_d. \tag{44}$$

The correct response is given by

$$y^*(k\Delta t) = y(k\Delta t) + \kappa_1(k\Delta t) + \kappa_2(k\Delta t), \tag{45}$$

where

$$\kappa_1(t) = \Delta y(0) r(t), \qquad \kappa_2(t) = \Delta\dot{y}(0) s(t), \tag{46}$$

such that in equation (29) one has $\kappa_1(k\Delta t) + \kappa_2(k\Delta t) = \Theta_0(k\Delta t)$.

TABLE 1

Frequencies (Hz) of free vibration of multi-span beam in Figure 5

Number of spans	Present study (D.S.M.) Mode number			Analytical solution [18] Mode number		
	1	2	3	1	2	3
1	0·5595	3·5068	9·918	0·5595	3·5068	9·820
2	0·3926	2·4538	3·534	0·3923	2·4494	3·526
3	0·3981	2·0266	2·921	0·3779	2·0284	2·919
4	0·3770	1·8432	2·453	0·3769	1·8430	2·455
5	0·3769	1·7499	2·185	0·3769	1·7500	2·185
6	0·3769	1·6968	2·019	0·3769	1·6966	2·020
7	0·3769	1·6640	1·911	0·3769	1·6635	1·911
8	0·3769	1·6424	1·837	0·3769	1·6430	1·838

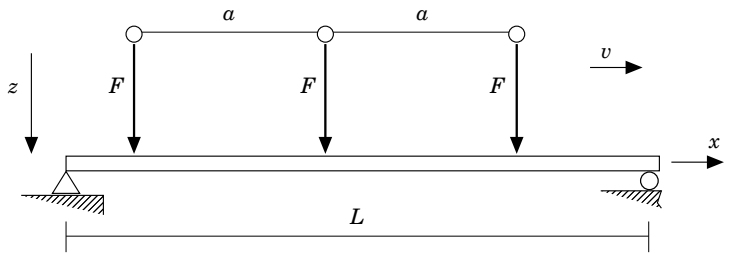

Figure 6. Beam under three moving forces with various values of distances a between forces.

The final solution is obtained by the mode superposition process:

$$w(x_r, t) = \sum_{j=1,nmode} \phi_{jr}(x_r) y_j^*(t), \tag{47}$$

where the number of modes (*nmode*) depends of the number of moving loads and the speed. One may consider ten to fifteen modes to evaluate displacements, velocities, accelerations and moments. More modes must be included in the analysis to evalute the shear forces.

4. NUMERICAL EXAMPLES

Three examples are presented which relate to beam structures under moving loads. The objectives of these examples are to demonstrate: (1) the precision of dynamic finite elements for evaluation of the frequencies of multi-span beam structures (example 1), (2) the precision of the dynamic modal approach coupled with a FFT to predict the response of single span (example 2) and multi-span structures (example 3) under a convoy of moving loads with various speeds.

4.1. FREE VIBRATIONS OF MULTI-SPAN BEAM-STRUCTURE

A beam-structure with multiple spans as shown in Figure 5 is considered. Equal length spans are added in order to evaluate the precision of frequencies estimated with the

TABLE 2

Properties and frequencies of a single span

	Properties	Mode number	Frequencies (Hz)
L	24·384 (m)	1	1·99
m_l	$9{\cdot}576 \times 10^3$ (kg/m)	2	7·99
A	0·594 (m^2)	3	17·99
I	$2{\cdot}95 \times 10^{-3}$ (m^4)	4	31·99
E	$19{\cdot}0 \times 10^{11}$ (N/m^2)	5	49·99
g	9·81 (m/s^2)	6	71·99
F	5324·256 (N)	7	97·99
v	22·5 (m/s)	8	127·99
		9	161·99
		10	199·99

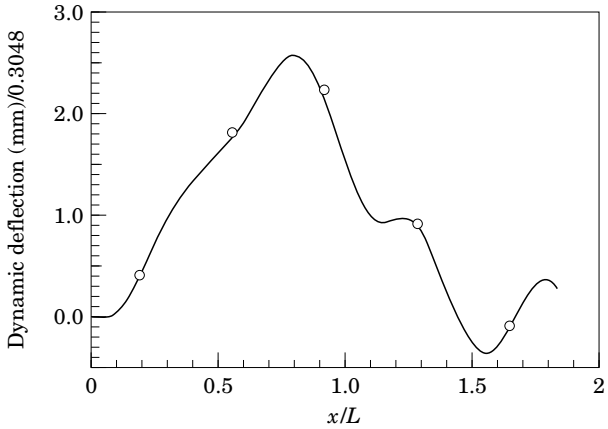

Figure 7. Dynamic vertical deflection at beam centre for different positions of moving loads $a = L/4$; one element; $v = 22{\cdot}5$ m/s; $x/L = vt/L$; ——, present study; ○, analytical solution.

dynamic element stiffness model (DSM) for various multi-span beams. One element is used for each span. The different parameters are defined in Figure 5. The analytic solution is given by Blevins [18] and results are compared in Table 1 for the first three modes and for span numbers varying from 1 to 8. As expected, the frequencies obtained by DSM have the same precision as the analytical values. This precision is maintained for every mode.

4.2. SINGLE SPAN BEAM UNDER A CONVOY OF MOVING LOADS

A one span beam under three moving loads (Figure 6) without dampling was studied. This example has been studied by Humar [4]. The properties of the structure are given in Table 2 with frequencies obtained by the dynamic stiffness model (DSM).

By using the model presented in the previous sections based on modal representation with DSM and FFT techniques, the dynamic response under three moving loads at constant velocity $v = 22{\cdot}5$ m/s has been studied. The analytic solution [8] is given as

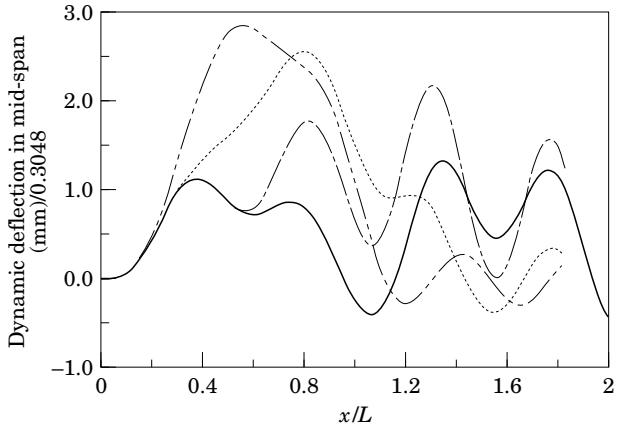

Figure 8. Dynamic vertical deflection at the centre of the beam for different values of a between the three moving loads; one element; $v = 22{\cdot}5$ m/s; $x/L = vt/L$; —··—, $a = L/8$; ·····, $a = L/4$; —·—, $a = L/2$; ——, $a = 1{\cdot}03 \times L$.

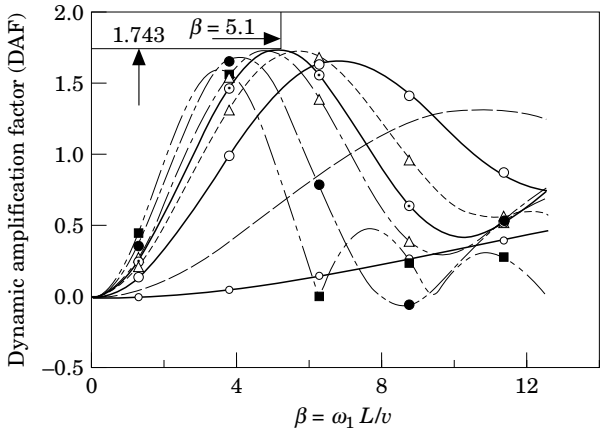

Figure 9. Variation of the DAF as a function of the velocities (β) and the positions of the load ($0 \leqslant \gamma = vt/L \leqslant 1$); solution at mid-span and with one moving-load. γ: —○—, 0·2; ——, 0·4; —◯—, 0·6; – –△– –, 0·7; —⊙—, 0·757; —–△—, 0·8; —●– –, 0·9; – –■—, 1·0.

follows:

$$w(x, t) = w_1(x, t) + w_2(x, t),$$

$$w_1(x, t) = \sum_{k=1}^{n_l} \left(\frac{2F_k}{m_l L} \sum_{j=1}^{\infty} \frac{\sin(j\pi x/L)}{(\omega_j^2 - \Omega_j^2)} \left\{ \sin(\Omega_j t_k) - \frac{\Omega_j}{\omega_j} \sin(\omega_j t_k) \right\} \right), \qquad \Omega_j = j\frac{\pi v}{L},$$

$$\text{if } 0 \leqslant t_k \leqslant L/v,\ 0 \leqslant \bar{x}_k = \bar{x}_1 - \sum_{l=1}^{k-1} a_l \leqslant L;$$

$$w_2(x, t) = \sum_{k=1}^{n_l} \sum_{j=1}^{N} \sqrt{\frac{2}{m_l L}} \left(y_j(\tau_k) \cos \omega_j(t_k - \tau_k) + \frac{\dot{y}_j(\tau_k)}{\omega_{jd}} \sin \omega_j(t_k - \tau_k) \right) \sin \frac{j\pi x}{L}$$

$$\text{if } \tau_k = \left(\sum_{l=1}^{k} a_{l-1} + L \right) \Big/ v, \qquad \bar{x}_k = \bar{x}_1 - \sum_{l=1}^{k-1} a_l \geqslant L;$$

n_l is the number of loads and a_i is the distance between forces F_i and F_{i-1}.

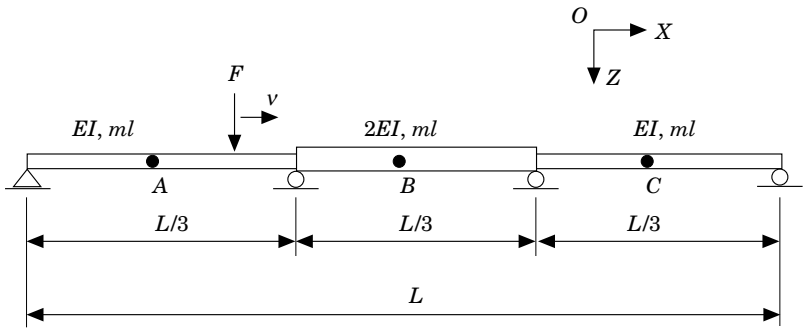

Figure 10. Three-span continuous beam with non uniform cross-section under moving force (3 elements, 4 nodes and 4 d.o.f.).

TABLE 3

Beam structure properties and natural frequencies

	Properties	Mode number	Frequencies (Hz)
L	60 (m)	1	6·204
ρ	$1{\cdot}0 \times 10^3$ (kg/m)	2	7·581
A	$0{\cdot}51 \times 10^{-2}$ (m^2)	3	11·974
EI	$1{\cdot}96 \times 10^9$ (N/m^3)	4	21·163
E	$10{\cdot}48 \times 10^{10}$ (N/m^2)	5	24·207
F	$9{\cdot}48 \times 10^3$ (N)	6	26·439
		7	37·282
		8	53·579
		9	56·642
		10	64·130

In this example, the choice of Δt is based on equation (35), with $f_{max} = f_5 = 49{\cdot}99$ Hz because the pulsation of a single moving load is given by (Biggs [19]): $f_{load} = v/2L = 0{\cdot}458 \text{ Hz} \leqslant f_5$. So $\Delta t = 1/2f_5 = 0.01$ s and $N = T/\Delta t = 2{\cdot}56 \text{ s}/0{\cdot}01 = 256$ steps.

In Figure 7, the deflection at mid-span for different times identified with the position of the first load is compared, remembering that only one element is used to discretize the structure. The initial values of displacement and velocity are zero.

The dynamic deflection at the centre of the beam under a moving convoy of three forces, for various values of distance a between forces, is shown in Figure 8. The results obtained are in agreement with the analytical solution [8] given previously. The results show the precision and reliability of the model developed in this study.

In the presented case of one moving load, the variation of the dynamic amplification factor DAF, defined as the maximum dynamic deflection divided by the maximum static deflection, is computed at the mid-span as a function of the position of the moving load and its velocity. Results are presented in Figure 9 and are in good agreement with analytic ones (Biggs [19]). One notes that the DAF is high and equal to 1·743 when $\tau = 0{\cdot}81T_1$, where $\tau = L/v$ (or in Figure 9, $\beta = \omega_1 L/v = 5{\cdot}1$). In this case $T_1 = 0{\cdot}5$ s (see Table 2), so $\tau = 0{\cdot}81 \times 0{\cdot}5 = 0{\cdot}405$ s and $v = 60{\cdot}207$ m/s. But for the false resonance (Biggs [19]) which is given by $\omega_{1structure} = \omega_{load} = \pi v/L$, the DAF is only equal to 1·54. In this case (see Table 2), $\omega_{1structure} = 4\pi$, so the velocity of the load is $v = 97{\cdot}536$ m/s.

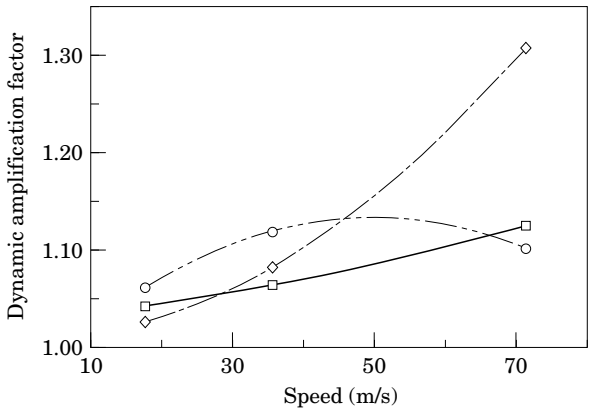

Figure 11. Relation between the dynamic amplification factor (DAF) and the velocity. DAF at: —◇—, A; —○– –, B; —□—, C.

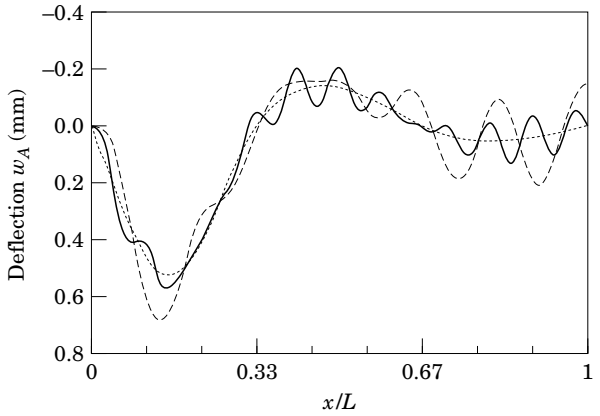

Figure 12. Dynamic and static vertical deflection at the centre of the first span: ——, $v = 35{\cdot}57$ m/s; – – –, $v = 71{\cdot}25$ m/s; - - - -, static.

4.3. THREE SPAN CONTINUOUS BEAM UNDER A MOVING FORCE

Finally, a multi-span beam under a moving load (Figure 10) is investigated. This example has been studied by Hayashikawa and Watanabe [2]. The structural properties and the values of the first ten frequencies are given in Table 3. By using the present dynamic stiffness-FFT model, we study the response for two speeds $v = 35{\cdot}57$ m/s and $v = 71{\cdot}25$ m/s, using one element per span (three elements for the bridge). In the example, the choice of Δt is based on equation (35), with $f_{max} = f_5 = 24{\cdot}207$ Hz because the pulsation of a single moving load is given by (Biggs [19]): $f_{load/span} = v/2L = 1{\cdot}78$ Hz $\leqslant f_5$. This gives $\Delta t = 1/2f_5 = 0{\cdot}02$ s and $N = T/\Delta t = 2{\cdot}56$ s/$0{\cdot}02 = 128$ steps.

In Figure 11, the influence of load speed on the amplification of displacement at three mid-points A, B and C of each span is presented. It can be seen that the first span mid-point is most sensitive to load speed and that the following points can be made: (1) the DAF increases for mid-points of first and last spans with higher velocities, while the maximum effect is in the first mid-point A; (2) the influence of velocity on the dynamic mid-point response of the middle span is not monotonous.

Figures 12 to 15 show the evolution of deflections at points A, B and C for different positions of the moving load. It can be seen that the behaviour of curves in Figures 12–15

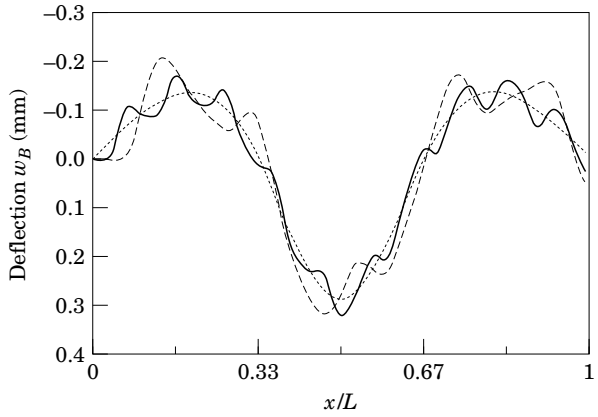

Figure 13. Dynamic and static vertical deflection at the centre of the second span: ——, $v = 35{\cdot}57$ m/s; – – –, $v = 71{\cdot}25$ m/s; - - - -, static.

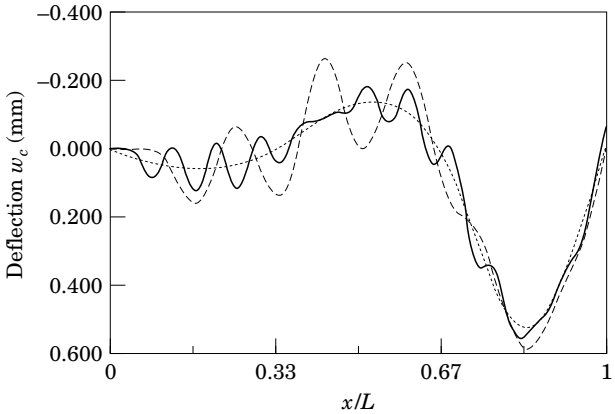

Figure 14. Dynamic and static vertical deflection at the centre of the third span: ——, $v = 35{\cdot}57$ m/s; – – –, $v = 71{\cdot}25$ m/s; - - - -, static.

and their extreme values are the same as those obtained by Hayashikawa and Watanabe [2].

5. CONCLUSION

In this study, a new model for evaluating the dynamic response of multi-span structures under a convoy of moving loads has been presented. The various aspects of this work are:

- presentation of a dynamic stiffness formulation within the framework of finite element approximation;
- construction of an uncoupled modal model using exact dynamic finite element eigenmodes;
- development of a model to predict the dynamic response employing a dynamic modal representation coupled with the FFT technique.

The practical applications of the present model show that the dynamic response can be captured in an exact way using only one element per span, because the dynamic

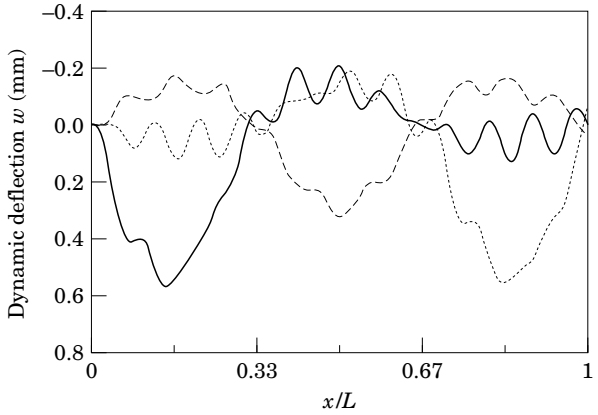

Figure 15. Dynamic vertical deflection at the points A, B and C with the velocity $v = 35{\cdot}57$ m/s: ——, w_A; – – –. w_B; - - - -, w_C.

interpolation functions N_i defined in equation (10) satisfy exactly the equilibrium equation (6) and, also, they are infinitely differentiable. The numerical solutions have, approximately, the same precision as those provided by the analytical solutions. The discretization error is related to the number of terms in the FFT and the number of modes retained. This formulation is valid whatever the speeds of the moving force and thus it is applicable for high speeds of the moving force. Also, it is applicable for short or long spans until the small deformation hypothesis becomes invalid. For the case of heavy moving masses, the formulation should be modified to take account of the coupling effect between the modal components in equation (25) because the true inertial effect of the moving mass should be included (Henchi *et al*. [20]).

REFERENCES

1. L. Fryba 1972 *Vibration of Solids and Structures under Moving Loads*. Groningen: Noordhoff International Publishing.
2. T. Hayashikawa and N. Watanabe 1981 *Journal of Structural Mechanics Division*, *American Society of Civil Engineers* **107**, 229–246. Dynamic behavior of continuous beams with moving loads.
3. R. W. Clough and J. Penzien 1993 *Dynamics of Structures*. New York: McGraw-Hill.
4. J. L. Humar 1990 *Dynamics of Structures*. Englewood Cliffs, New Jersey: Prentice Hall.
5. R. S. Ayer, G. Ford and L. S. Jacobsen 1950 *Journal of Applied Mechanics* **3,** 1–12. Transverse vibration of two span beam under action of moving constant forces.
6. A. S. Veletsos and T. Huang 1970 *Journal of Engineering Mechanics Division*, *American Society of Civil Engineers* **90**, 1648–1659. Analysis of dynamic response of highway bridges.
7. J. W. Cooley and J. W. Tukey 1965 *Mathematical Computation* **19**, 297–301. An algorithm for the machine calculation of complex Fourier series.
8. K. Henchi 1995 *Dynamic analysis of bridges under moving vehicles by a finite element method*. Ph.D. thesis, Université de Technologie de Compiègne, France (In French).
9. J. L. Humar and H. Xia 1993 *Earthquake Engineering Structural Dynamics* **22**, 1–12. Dynamic response analysis in the frequency domain.
10. J. R. Banerjee 1989 *International Journal of Numerical Methods in Engineering* **28**, 1283–1298. Coupled bending-torsional dynamic stiffness matrix for beam element.
11. P. O. Friberg 1983 *International Journal for Numerical Methods in Engineering* **19**, 479–493. Coupled vibrations of beams—an exact dynamic element stiffness matrix for beam.
12. K. Henchi, H. Badraoui, G. Dhatt and D. Seligmann 1994 *Non-Linear Calculation of the Eigenvalues by the Dynamic Stiffness Matrices Approach*. Report No 01/94 EDF-Université de Technologie de Compiègne, France (In French).
13. G. Dhatt and G. Touzot 1981 *Finite Element Displayed*. New York: John Wiley.
14. K. J. Bathe 1976 *Numerical Methods in Finite Element Analysis*. Englewood Cliffs, New Jersey: Prentice Hall.
15. A. Y. T. Leung 1979 *International Journal of Numerical Methods in Engineering* **12**, 1705–1716. An accurate method of dynamic substructuring with simplified computation.
16. F. W. Williams and W. H. Wiltrick 1971 *Quarterly Journal of Mechanics and Applied Mathematics* **24**, 263–284. A general algorithm for computing natural frequencies of elastic structures.
17. W. P. Howson 1979 *Advances in Engineering Software*, **1**, 181–190. A compact method for computing the eigenvalues and eigenvectors of plane frame.
18. R. D. Blevins 1979 *Formulas for Natural Frequencies and Model Shapes*. Reinhold, New York: Van Nostrand.
19. J. M. Biggs 1964 *Introduction to Structural Dynamics*. New York: McGraw-Hill.
20. K. Henchi, G. Dhatt, M. Talbot and M. Fafard 1996 *European Journal of Finite Elements*. Dynamic analysis of continuous beams under moving forces and masses. A semi-analytical and finite elements approach. (In French). (submitted)

APPENDIX A: DYNAMIC STIFFNESS MATRIX OF BERNOULLI-EULER BEAM

The development of the equation (13) gives the exact following dynamic stiffness matrix:

$$[\mathrm{k}_d(\alpha)] = \frac{EI}{L^3(1-cC)} \begin{bmatrix} k_{d_{1,1}} & k_{d_{1,2}} & k_{d_{1,3}} & k_{d_{1,4}} \\ & k_{d_{2,2}} & k_{d_{2,3}} & k_{d_{2,4}} \\ & & k_{d_{3,3}} & k_{d_{3,4}} \\ \text{Sym.} & & & k_{d_{4,4}} \end{bmatrix},$$

where

$$k_{d_{1,1}} = \alpha^3 L^3(Cs + Sc), \qquad k_{d_{2,2}} = \alpha L^3(Cs + Sc), \qquad k_{d_{1,2}} = \alpha^2 L^3 Ss,$$
$$k_{d_{2,3}} = \alpha^2 L^3(C - c), \qquad k_{d_{1,3}} = \alpha^3 L^3(s + S), \qquad k_{d_{2,4}} = \alpha L^3(S - s),$$
$$k_{d_{1,4}} = \alpha^2 L^3(C - c), \qquad k_{d_{3,3}} = \alpha^3 L^3(Cs + Sc), \qquad k_{d_{4,4}} = \alpha L^3(Cs + Sc),$$
$$k_{d_{3,4}} = -\alpha^2 L^3 Ss,$$

and where $c = \cos \alpha L$, $s = \sin \alpha L$, $C = \cosh \alpha L$ and $S = \sinh \alpha L$.

APPENDIX B: NOTATION

A	cross-section of the beam
$\delta(x - \bar{x}_k)$	Dirac delta function at position $x = \bar{x}_k$
Δt, Δt_{cr}	time step and critical time step
EI	flexural stiffness
$\phi_{rn}(x_r)$	eigenfunction of mode n relative to the span r
$\Phi_n(X_r)$	eigenfunction of mode n relative to the total continuous structure
$F_k(t)$	kth moving load
l_r; L_T	length of the rth span and total length of the continuous beam
$[\mathrm{K}(\omega^2)]$;	dynamic stiffness matrix
$[\mathrm{M}(\omega^2)]$	dynamic mass matrix
$N_i(\alpha, x)$	dynamic shape function i
n_l	number of loads present on the bridge
$\langle N \rangle$	vector of dynamic shape functions
$P_f(\Omega)$	generalised load in frequency domain
$p_j(t)$	generalised load of mode j
m_l	mass per unit of length
T_j, f_j, ω_j	period, frequency and pulsation of the mode j
T	period of excitation
$y_m, \dot{y}_m, \ddot{y}_m$	modal displacement, velocity and acceleration of mode m
$Y_f(\Omega)$	modal solution in frequency domain
$\forall x$	whatever the value of x
$\{\mathrm{U}_n\}$	vector of the system global displacements
$\{w_n\}$	element local nodal displacements